doi: 10.1017/S1431927609094598
Microsc Microanal 15(Suppl 2), 2009

Convenient Electron Optics set up for Zernike Phase Microscopy in TEM

Masahiro Kawasaki[#], Marek Malac*, Peng Li[*], Hui Qian[*], Ray Egerton[*]

[#] JEOL USA, 11 Dearborn Road, Peabody , MA, 01960, USA.
[*] National Institute of Nanotechnology, 11421 Saskatchewan Drive, Edmonton, Canada.

Radiation damage sets the ultimate limit for analysis in an electron microscope. The damage is often directly proportional to irradiation dose (measured in $e^-/Å^2$) applied to the sample. A Zernike phase plate (ZPP) can reduce the irradiation dose needed to obtain a desired signal/noise ratio (SNR) [1]. Traditionally the Zernike phase plate is positioned in the back focal plane of the objective lens. The limited space within the polepiece gap of the objective lens poses significant challenges for practical implementation of ZPP in the TEM. A transfer lens can be inserted in the TEM column, requiring the design of the microscope to be modified [2], but here we report a convenient electro-optical setup that transfers the back focal plane of the objective lens to the selected-area aperture (SAA) plane using the standard objective mini lens. A ZPP can be then conveniently located in the SAA plane of the microscope without the need for an additional transfer lens.

Figure 1 schematically shows the electro-optical setup. The set up is similar to that used for medium magnification electron holography experiments [3]. The back focal plane of the objective lens is transferred from within the gap of the objective lens to SAA plane. The physical dimensions of the free space available in the SAA plane vary between manufacturers but can be of the order of 10 mm along the beam path, while the size of the port for SAA is often 10 mm in diameter. We have used an electron-beam evaporated carbon film ZPP [4] rather than electrostatic ZPP [5] to demonstrate the suitability of our setup for ZPP imaging. The diameter of the opening in the carbon film was between 50 nm and 500 nm in our experiments. The carbon film thickness estimated during deposition by a thickness monitor was about 40 nm.

Figure 2 shows a diffraction pattern at the SAA plane with the ZPP inserted. The Bragg reflection marked by an arrow is from 0.34 nm lattice planes of a multiwall carbon nanotube, allowing us to assess the angular size of the *cut on* semi-angle of the ZPP. In this particular case the *cut on* semi-angle was 0.1 mrad, corresponding to transfer of up to 0.04 nm^{-1} (or 24 nm) through the ZPP opening. Spatial frequencies higher than 0.04 nm^{-1} are phase shifted by the ZPP. The convergence semi angle of the incident 200 kV Koehler illumination beam used in our experiments is about 0.04 mrad, measured as the full width half maximum of the diffracted beams in Figure 2. It is desirable for the thickness (phase shift) of the ZPP to be about one quarter of a wavelength or $\pi/2$. The thickness can be assessed from contrast transfer phase functions with and without ZPP, shown in Figure 3a and Figure 3b respectively or by electron holography. The phase shift of the ZPP used in our experiments was measured as $\Phi = (3.3 \pm 0.1)$ rad by electron holography, too high for Zernike contrast imaging but sufficient to demonstrate the ability to bring the back focal plane of the objective lens to the selected area aperture plane using an objective minilens. The electro-optical set up that we demonstrated can accommodate magnification at the slow-scan camera plane from a few thousand times to about 90,000x in our Jeol 2200 FS TEM equipped with a cryo polepiece and in column filter. This magnification range corresponds to a camera pixel size from about 2 nm to about 0.1 nm, a good match with the desired pixel size for most experiments on organic materials. The magnification at the film plane is about 20% less than at the slow-scan camera plane. In a microscope with post-column

energy filter, such as GIF, the magnification would increase by a factor of about 10x leading to maximum magnification of about 900,000x.

Figures 4a) and 4b) show images of a sample of Pt/Ru nanoparticles on multiwall carbon nanotubes, with and without ZPP in the electro-optical path. The in-column filter of the JEOL 2200 FS additionally allows for energy filtering of the data. Both Figure 3 and Figure 4 were acquired with an energy selecting slit (width 20 eV) centered at the zero loss peak. The ringing in Figure 4a may be due to the small size of the ZPP opening in a very thick (3 rad) ZPP.

[1] Malac M, Beleggia M, Egerton RF, Zhu Y, Ultramicroscopy 108 (2008), 126.
[2] Hosokawa et al, Journal of Electron Microscopy 54 (2005), p. 317.
[3] Wang YY, Kawasaki M et al, Ultramicroscopy 101, 63.
[4] Nagayama K, Danev R, US patent 20080202918 A1.
[5] Chen KF et al, Micron 39 (2008), 749.
[6] The support for this work was provided by NINT/NRC and by JEOL USA (M.K.).

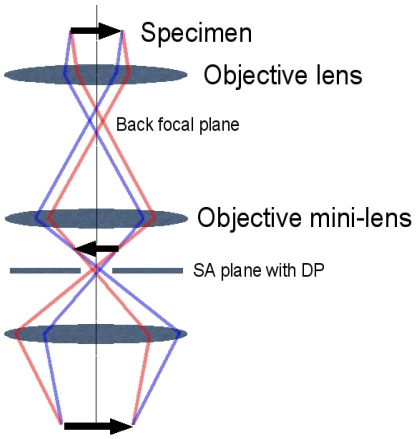

Fig. 1. Schematic drawing of electron optics allowing transfer of the back focal plane of the objective lens to the selected area aperture plane of a TEM.

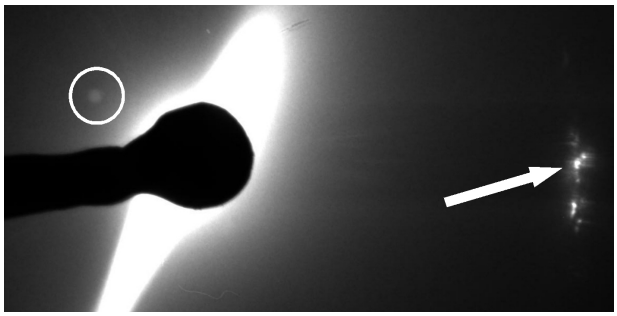

Fig. 2. Diffraction pattern collected from multiwall carbon nanotubes with Pt/Ru catalysts. The Bragg spot marked by an arrow corresponds to 0.34 nm lattice planes. The ZPP opening marked by a circle is 0.2 mrad corresponding to *cut on* frequency of 0.04 nm^{-1}.

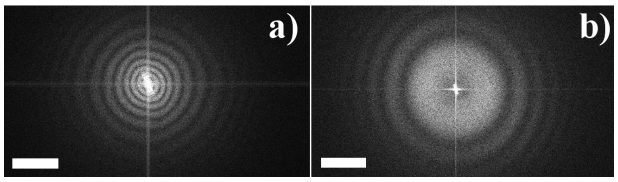

Fig. 3. Phase contrast transfer function with ZPP (a) and without ZPP (b) in the beam path. The under focus is about 780 nm in (b) and nearly 8000 nm in (a) . The scale bar corresponds to 0.6 nm^{-1}.

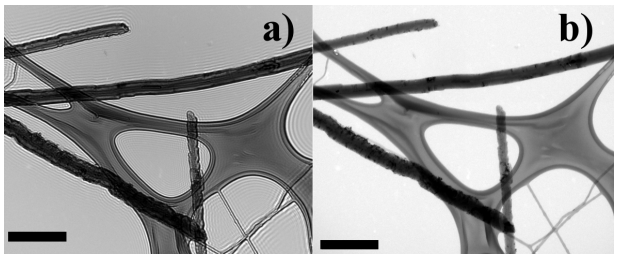

Fig. 4. Image of sample with multiwall carbon nanotubes with Pt/Ru catalyst nanoparticles. a) with ZPP in the beam path and b) without ZPP in the beam path. The scale bar is 500 nm.

https://doi.org/10.1017/S1431927609094598 Published online by Cambridge University Press